

## Photoluminescence and Optical Waveguiding Characteristics of Bisalkoxy Tin(IV) Porphyrin Microcrystals

Seong-Gi Jo,<sup>[a]</sup> Sundol Kim,<sup>[b]</sup> Eun Hei Cho,<sup>[a]</sup> Da Hee Lee,<sup>[b]</sup> Jeongyong Kim,<sup>[c]</sup> Suk Joong Lee,<sup>\*[b]</sup> and Jinsoo Joo<sup>\*[a]</sup>

During the last decade, many efforts have been focused on the fabrication of nano- and microstructured functional materials because of their potential applications as building blocks for miniaturized photonics, electronics, and sensors.<sup>[1–3]</sup> In particular, inorganic and organic nano- and microrods have been studied for optical waveguiding materials, which show efficient propagation and manipulation of incident light signal on the subwavelength scale.<sup>[4–6]</sup> Recently, it was realized that one-dimensional nano- and microrod structures using polymers<sup>[7]</sup> and organic molecules<sup>[8–12]</sup> could serve as effective building blocks to generate and propagate light in the future miniaturized photonics. In addition, organic semiconducting microcrystals<sup>[13,14]</sup> have unique photonic and electronic properties,<sup>[15,16]</sup> because of the  $\pi$ - $\pi$  intermolecular interactions<sup>[17]</sup> and high luminescence efficiency.

Porphyrin and metalloporphyrins have received considerable attention because of their photostability, high visible extinction coefficient, and electron-transfer properties,<sup>[18–20]</sup> which contributed to their use as active materials for charge transport, photoelectronic conversion, nonlinear optics, organic light-emitting diodes, organic photovoltaic cells, and optical information storage.<sup>[21–24]</sup> Recently, the self-assembly of porphyrin-based nanostructures, including nanoporous solid materials, have been intensively studied.<sup>[25–27]</sup> However, the nanoscale luminescence and optical waveguiding characteristics of metalloporphyrin-based microcrystals with various morphologies have not been thoroughly investigated.

In this study, we investigated the nanoscale photoluminescence (PL) and optical waveguiding characteristics of bisal-

koxo tin(IV) porphyrin based microcrystalline rods and plates using a laser confocal microscope (LCM) system. These microcrystals were prepared from slow diffusion of solutions of bisalkoxy tin(IV) porphyrin **1** and **2** in respective alcohols (*n*-propanol for (porphyrin)Sn(OPr)<sub>2</sub> (**1**) and isopropyl alcohol for (porphyrin)Sn(O*i*Pr)<sub>2</sub> (**2**)) over water. We observed that the single-crystal structures and morphology of microcrystals of **1** and **2** are clearly different. The LCM-PL peaks of single microcrystals of **1** and **2** were observed at 635 nm when they were excited at 488 nm, which is considerably different from their solution PL. From optical waveguiding experiments using the LCM system, the efficiency of optical waveguiding for the microcrystalline rod of **1** was five times better than that for **2**, because of the relatively strong  $\pi$ - $\pi$  intermolecular interaction along the main crystalline axis.

Figure 1 shows the single-crystal structures and packing diagrams of **1** and **2**. The porphyrin cores in both **1** and **2** are nearly planar. Two phenyl rings are tilted relative to the porphyrin plane by tilting angles of 78.8(2)° for **1** and 72.9(4)° and 80.8(3)° for **2**. In **1**, two propanol molecules axially coordinate to a Sn<sup>IV</sup> ion (Figure 1a), but in **2**, isopropyl alcohol molecules did not coordinate to a Sn<sup>IV</sup> ion; instead, two water molecules coordinate to a Sn<sup>IV</sup> ion (Figure 1b). Two isopropyl alcohol molecules have been liberated during the crystal growth. Figure 1c,e,f and Figure 1d,g,h show the difference in packing patterns of the two compounds, and it might be consistent with each crystal type (rod for **1** and plate for **2**). These molecules show clear slip-stack arrangement of the porphyrin planes (Figure 1e–h) and interacted through  $\pi$ - $\pi$  interactions (3.035 Å for **1** and 3.328 Å for **2**).

Figure 2 shows CCD images of microcrystals made of **1** and **2**, and the insets show SEM images of the corresponding microcrystals. The microcrystal of **1** shows a thickness of 2–3  $\mu$ m and length of approximately 50  $\mu$ m. For **2**, the thickness was approximately 200 nm, the width 14  $\mu$ m, and the length 19  $\mu$ m. The red light emission was dominant for both microcrystals.

Figure S4a in the Supporting Information shows UV/Vis absorption spectra of **1** and **2**, in both solution and solid states. All samples show a sharp and strong Sorét band corresponding to S<sub>0</sub>→S<sub>2</sub> transition and a set of weak Q-bands due to S<sub>0</sub>→S<sub>1</sub> transition, which are typical absorption profiles for porphyrin-based compounds.<sup>[28,29]</sup> However, drastic spectral changes were observed in the crystal state, which is

[a] S.-G. Jo, E. H. Cho, Prof. J. Joo  
Department of Physics, Korea University  
Seoul 136-713 (South Korea)  
Fax: (+82)2-927-3292  
E-mail: jjoo@korea.ac.kr

[b] S. Kim, D. H. Lee, Prof. S. J. Lee  
Department of Chemistry, Korea University  
Seoul 136-713 (South Korea)  
Fax: (+82)2-925-4284  
E-mail: slee1@korea.ac.kr

[c] Prof. J. Kim  
Department of Physics, University of Incheon  
Incheon 406-772 (South Korea)

Supporting information for this article is available on the WWW under <http://dx.doi.org/10.1002/asia.201200749>.

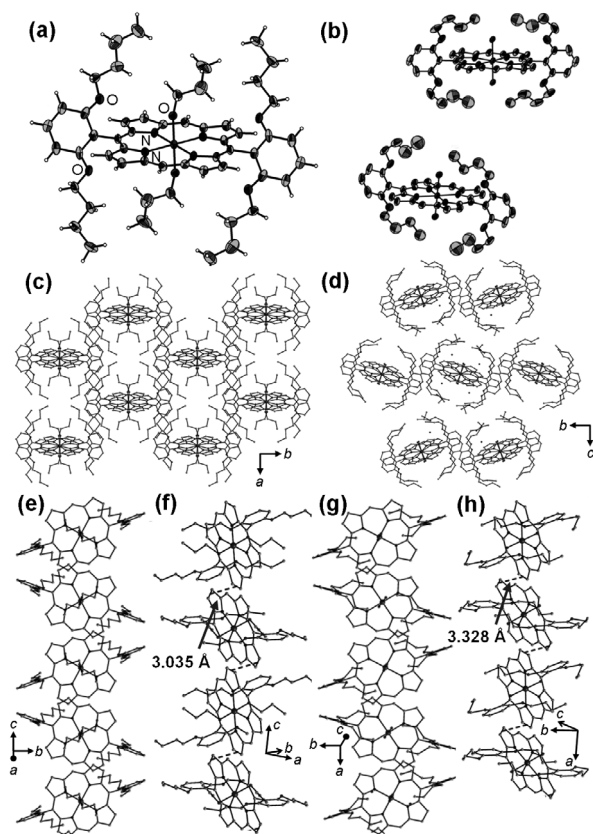


Figure 1. Single-crystal X-ray structures and packing diagram representations of **1** (a, c, e, and f) and **2** (b, d, g, and h).

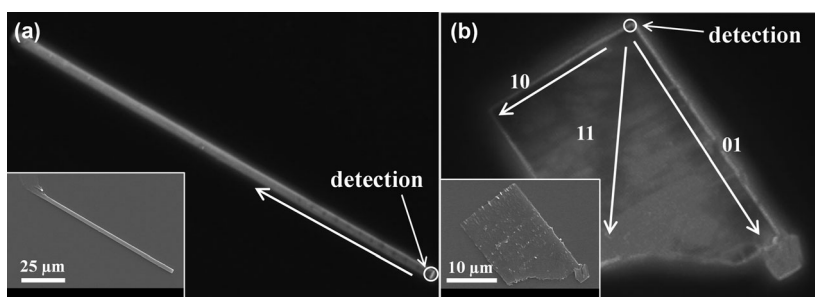


Figure 2. CCD images of microcrystals of a) **1** and b) **2**. The white circles represent the detecting positions for optical waveguiding experiments. The arrows represent moving directions of the input laser. Insets: SEM images of the corresponding microcrystals.

attributed to the intermolecular interaction between the tin(IV) porphyrins. For example, the solution samples of **1** and **2** exhibit Sorét bands at 415 nm with Q-bands around 548 nm, while the absorption spectra of microcrystals of **1** and **2** show broadened and slightly red-shifted Sorét bands at 420 nm and Q-bands around 552 nm. The PL spectra of the solution samples of **1** and **2** show identical emission bands at 590 and 644 nm, while a band at 638 nm, indicating red-light emission,<sup>[16]</sup> with weak satellite peaks at 606, 660, and 700 nm is observed for the LCM-PL of the microcrystals of **1** and **2** (Figure S4b). These findings indicate a high degree of intermolecular interaction between the porphyrin units upon crystal formation.

Figure 3a shows a schematic illustration of the optical waveguiding experiment using a microcrystalline rod of **1** and the LCM system. Note that the propagation distance of focused incident light was varied through a movable input laser. Figure 3b shows the variation of output LCM-PL spectra depending on the propagation distance for a microcrystalline rod sample of **1**. The insets of Figure 3 are the LCM-PL spectra of microcrystals for the reference, that is, the PL spectra in the same input and output positions. As the propagation distance of the input light increased, the LCM-PL intensity at 638 nm modestly decreased for a microcrystalline rod of **1** (Figure 3b), while that for **2** rapidly decreased (Figure 3c–e). These results imply that the microcrystalline rod of **1** has better optical signal transporting characteristics than the microcrystalline plate of **2**. Furthermore, the output LCM-PL peaks for microcrystalline rod of **1** were red-shifted from 638 to 652 nm.

The output LCM-PL spectra of microcrystalline plate of **2** varied with the propagation directions of the incident light, as shown in Figure 3c–e. The output LCM-PL intensities along the 01 direction (i.e., the major crystal growing axis) in the microcrystalline plate of **2** were the most weakly decreased with increasing the propagation distance (Figure 3c), while those along the 10 direction (i.e., the direction perpendicular to the major crystal growing direction in the same plane) were strongly reduced and those along the 11 direction (diagonal) were intermediately decreased.

To quantitatively analyze optical waveguiding characteristics of the microcrystals of **1** and **2**, the output LCM-PL intensities at 638 nm were plotted as a function of the propagation distance of input light (Figure 4). The output LCM-PL intensities of the waveguided light decayed exponentially. Therefore, we used the equation  $I(x) = I_0 e^{-\alpha x}$ , in which  $I$  is the output LCM-PL intensity,  $I_0$  is the proportional constant of the intensity,  $\alpha$  is the decay constant in the unit of  $\mu\text{m}^{-1}$ , and  $x$  is the propagation distance of the incident light. From the slope in Figure 4, the decay constant  $\alpha$  was estimated to be about  $0.040 \mu\text{m}^{-1}$  for the microcrystalline rod of **1**. However, the  $\alpha$  values of microcrystalline plate of **2** were 0.198, 0.258, and  $0.428 \mu\text{m}^{-1}$  along the 01, 11, and 10 directions, respectively. These results imply that the microcrystalline rod of **1** has better optical waveguiding characteristics than the microcrystalline plate of **2**. Clearly, the  $\pi$ - $\pi$  stacking of tin(IV) porphyrin molecules took place along the  $c$  axis (major crystal growing direction) with a layer distance of 3.035 Å, which was assigned as the longitudinal direction of the microcrystalline rod of **1** (Figure 1). For the microcrystalline plate of **2**, the waveguiding efficiency varied with the propagation direction, because the anisotropic molecular arrangement de-

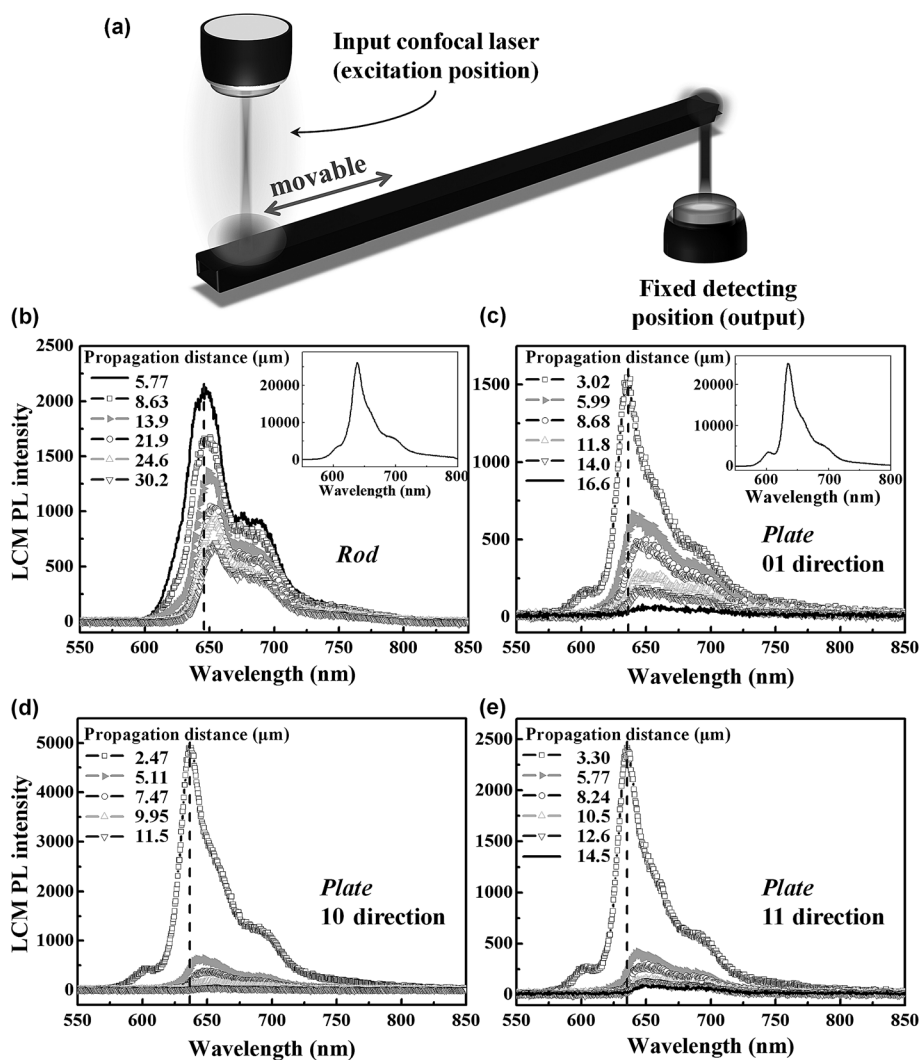


Figure 3. a) Schematic representation of optical waveguiding experiment using a microcrystalline rod of **1** and the LCM system. b) Output LCM-PL spectra of the microcrystalline rod of **1** with various propagation distances. c–e) Output LCM-PL spectra of the microcrystalline plate of **2** along the 01 (c), 10 (d), 11 (e) directions. Insets: LCM-PL spectra measured at the same input and output position for the reference.

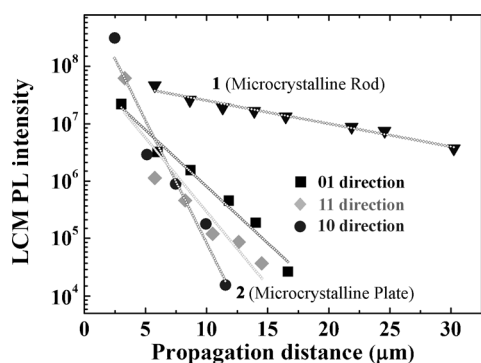


Figure 4. Plot of LCM-PL intensity versus propagation distance of input light for microcrystals of **1** and **2**.

pendent on the crystalline axis. Presumably the longer direction (01 direction) of the microcrystal sample of **2** is the main  $\pi$ - $\pi$  stacking direction, corresponding to the  $a$  axis

with a stacking distance of 3.328 Å (Figure 1), resulting in the weaker decay constant. Therefore, we suggest that the optical waveguiding can be efficient along the  $\pi$ - $\pi$  stacking direction of tin(IV) porphyrin molecules, and the decay constants are highly depending on the  $\pi$ - $\pi$  stacking distances and directions.

Bisalkoxy tin(IV) porphyrin based microcrystals were fabricated by a slow diffusion method to give rods for **1** and plates for **2**. We observed the characteristic optical peaks of the tin(IV) porphyrin microcrystals from the UV/Vis absorption and LCM-PL spectra. From the optical waveguiding experiments, the decay constant of LCM-PL intensity for the microcrystalline rod of **1** was estimated to be  $0.040 \mu\text{m}^{-1}$ , which was more efficient than that of the microcrystalline plate of **2**. This drastic change in the efficiency of optical signal transport is due to the well-aligned  $\pi$ - $\pi$  stacking of tin(IV) porphyrin molecules along the longitudinal direction and close packing distance of **1** in microcrystal. In the microcrystalline plate of **2**, anisotropic optical waveguiding was observed, which was due to the anisotropic  $\pi$ - $\pi$  interaction and different molecular arrangement depending on the crystalline direction.

## Experimental Section

### Crystal data for **1**

$\text{C}_{60}\text{H}_{70}\text{N}_4\text{O}_{10}\text{Sn}$ , MW = 1125.89, orthorhombic (space group  $Pbcn$ ),  $a = 14.420(3)$ ,  $b = 22.624(5)$ ,  $c = 15.891(3)$  Å,  $V = 5184.3(18)$  Å<sup>3</sup>,  $Z = 4$ , (Mo  $K\alpha$ ) =  $0.559 \text{ mm}^{-1}$ , 28 314 reflections measured, 5099 unique ( $R_{\text{int}} = 0.1346$ ), which were used in all calculations, final  $R = 0.0786$  ( $R_w = 0.2125$ ) with reflections having intensities greater than  $2\sigma$ , GOF ( $F^2$ ) = 0.974.

### Crystal data for **2**

$\text{C}_{54}\text{H}_{41}\text{N}_4\text{O}_{10}\text{Sn}$ , MW = 1024.60, monoclinic (space group  $P2_1/c$ ),  $a = 15.078(3)$ ,  $b = 14.111(3)$ ,  $c = 28.016(6)$  Å,  $\beta = 95.19(3)^\circ$ ,  $V = 5936(2)$  Å<sup>3</sup>,  $Z = 4$ , (Mo  $K\alpha$ ) =  $0.482 \text{ mm}^{-1}$ , 32 571 reflections measured, 11 634 unique ( $R_{\text{int}} = 0.0947$ ), which were used in all calculations, final  $R = 0.0813$  ( $R_w =$

0.2161) with reflections having intensities greater than  $2\sigma$ , GOF ( $F^2$ ) = 0.967.

CCDC 888057 (1) and CCDC 888056 (2) contain the supplementary crystallographic data for this paper. These data can be obtained free of charge from the Cambridge Crystallographic Data Centre via [www.ccdc.cam.ac.uk/data\\_request/cif](http://www.ccdc.cam.ac.uk/data_request/cif).

### Acknowledgements

This study was supported by the Korea Science and Engineering Foundation (KOSEF) grant (No. 2012R1A2A2A01045102), Korea Research Foundation Program (NRF-20120002285) and Priority Research Centers Program (NRF-20120005860) through the National Research Foundation of Korea (NRF) funded by the Korean government (MEST).

**Keywords:** luminescence • optical waveguides •  $\pi$ - $\pi$  interactions • porphyrinoids • tin

- [1] H. Kind, H. Yan, B. Messer, M. Law, P. Yang, *Adv. Mater.* **2002**, *14*, 158–160.
- [2] J. Wang, M. S. Gudixsen, X. Duan, Y. Cui, C. M. Lieber, *Science* **2001**, *293*, 1455–1457.
- [3] Z. L. Wang, *Adv. Mater.* **2003**, *15*, 432–436.
- [4] P. Yang, H. Yan, S. Mao, R. Russo, J. Johnson, R. Saykally, N. Morris, J. Pham, R. He, H.-J. Choi, *Adv. Funct. Mater.* **2002**, *12*, 323–331.
- [5] Q. Liao, H. Fu, J. Yao, *Adv. Mater.* **2009**, *21*, 4153–4157.
- [6] A. B. Greytak, C. J. Barrelet, Y. Li, C. M. Lieber, *Appl. Phys. Lett.* **2005**, *87*, 151103.
- [7] D. O'Carroll, I. Lieberwirth, G. Redmond, *Small* **2007**, *3*, 1178–1183.
- [8] K. Takazawa, Y. Kitahama, Y. Kimura, G. Kido, *Nano Lett.* **2005**, *5*, 1293–1296.
- [9] X. Yan, J. Li, H. Möhwal, *Adv. Mater.* **2011**, *23*, 2796–2801.
- [10] Y. S. Zhao, A. Peng, H. Fu, Y. Ma, J. Yao, *Adv. Mater.* **2008**, *20*, 1661–1665.
- [11] X. Yan, Y. Su, J. Li, J. Früh, H. Möhwal, *Angew. Chem.* **2011**, *123*, 11382–11387; *Angew. Chem. Int. Ed.* **2011**, *50*, 11186–11191.
- [12] X. Yan, P. Zhu, J. Li, *Chem. Soc. Rev.* **2010**, *39*, 1877–1890.
- [13] Y. S. Zhao, C. Di, W. Yang, G. Yu, Y. Liu, J. Yao, *Adv. Funct. Mater.* **2006**, *16*, 1985–1991.
- [14] Y. S. Zhao, H. Fu, F. Hu, A. Peng, W. Yang, J. Yao, *Adv. Mater.* **2008**, *20*, 79–83.
- [15] K. Balakrishnan, A. Datar, R. Oitker, H. Chen, J. Zuo, L. Zang, *J. Am. Chem. Soc.* **2005**, *127*, 10496–10497.
- [16] J. K. Lee, W. K. Koh, W. S. Chae, Y. R. Kim, *Chem. Commun.* **2002**, 138–139.
- [17] Y. S. Zhao, W. Yang, D. Xiao, X. Sheng, X. Yang, Z. Shuai, Y. Luo, J. Yao, *Chem. Mater.* **2005**, *17*, 6430–6435.
- [18] J. Sokolnicki, R. Wiglus, S. Radzki, A. Graczyk, J. Legendziewicz, *Opt. Mater.* **2004**, *26*, 199–206.
- [19] R. Wiglus, J. Legendziewicz, A. Graczyk, S. Radzki, P. Gawryszewska, J. Sokolnicki, *J. Alloys Compd.* **2004**, *380*, 396–404.
- [20] C. Von Borczyskowski, U. Rempel, E. Zenkevich, A. Shul'ga, A. Chernook, *Chem. Sci.* **1995**, *107*, 803–811.
- [21] F. J. Kampas, M. Gouterman, *J. Phys. Chem.* **1977**, *81*, 690–695.
- [22] C.-y. Liu, H.-l. Pan, M. A. Fox, A. J. Bard, *Chem. Mater.* **1997**, *9*, 1422–1429.
- [23] V. S.-Y. Lin, S. G. DiMagno, M. J. Therien, *Science* **1994**, *264*, 1105–1111.
- [24] R. W. Wagner, J. S. Lindsey, J. Seth, V. Palaniappan, D. F. Bocian, *J. Am. Chem. Soc.* **1996**, *118*, 3996–3997.
- [25] A. D. Schwab, D. E. Smith, C. S. Rich, E. R. Young, W. F. Smith, J. C. de Paula, *J. Phys. Chem. B* **2003**, *107*, 11339–11345.
- [26] X. Shi, K. M. Barkigia, J. Fajer, C. M. Drain, *J. Org. Chem.* **2001**, *66*, 6513–6522.
- [27] T. van der Boom, R. T. Hayes, Y. Zhao, P. J. Bushard, E. A. Weiss, M. R. Wasielewski, *J. Am. Chem. Soc.* **2002**, *124*, 9582–9590.
- [28] F.-L. Jiang, D. Fortin, P. D. Harvey, *Inorg. Chem.* **2010**, *49*, 2614–2623.
- [29] A. Lukaszewicz, J. Karolczak, D. Kowalska, A. Maciejewski, M. Ziolk, R. P. Steer, *Chem. Phys.* **2007**, *331*, 359–372.

Received: August 16, 2012  
Published online: October 2, 2012